Article:

BIOTECHNOLOGY
BIOENGINEERING WILEY

Biomimetic surface delivery of NGF and BDNF to enhance neurite outgrowth

Ana M. Sandoval-Castellanos | Frederik Claeyssens | John W. Haycock ⓘ

Department of Materials Science and Engineering, The University of Sheffield, Sheffield, United Kingdom

Correspondence
John W. Haycock, Department of Materials Science and Engineering, The University of Sheffield, Sir Robert Hadfield Building, Mappin Street, Sheffield S1 3JD, United Kingdom.
Email: j.w.haycock@sheffield.ac.uk

Funding information
Consejo Nacional de Ciencia y Tecnología

Abstract

Treatment for peripheral nerve injuries includes the use of autografts and nerve guide conduits (NGCs). However, outcomes are limited, and full recovery is rarely achieved. The use of nerve scaffolds as a platform to surface immobilize neurotrophic factors and deliver locally is a promising approach to support neurite and nerve outgrowth after injury. We report on a bioactive surface using functional amine groups, to which heparin binds electrostatically. X-ray photoelectron spectroscopy analysis was used to characterize the presence of nitrogen and sulfur. Nerve growth factor (NGF) and brain-derived neurotrophic factor (BDNF) were bound by electrostatic interaction to heparin, and the release profile evaluated by enzyme-linked immunosorbent assay, which showed that ca. 1% of NGF was released from each of the bioactive surface within 7 days. Furthermore, each surface showed a maximum release of 97% of BDNF. Neurotrophin release on neurite outgrowth was evaluated by primary dorsal root ganglion with a maximum neurite growth response in vitro of 1,075 μm detected for surfaces immobilized with NGF at 1 ng/ml. In summary, the study reports on the design and construction of a biomimetic platform to deliver NGF and BDNF using physiologically low concentrations of neurotrophin. The platform is directly applicable and scalable for improving the regenerative ability of existing NGCs and scaffolds.

KEYWORDS
bioactive surface, brain-derived neurotrophic factor, nerve growth factor, nerve repair, neurite outgrowth

1 | INTRODUCTION

Peripheral nerve injury is a major cause of disability, affecting 1 in 1,000 patients (Hughes, 2008). Injuries drastically affect life quality and health due to decreased sensory and motor function (Daly, Yao, Zeugolis, Windebank, & Pandit, 2012; Lundborg, 2003; Pateman et al., 2015). Self-regeneration may occur if the injury is not severe. However, as the degree of injury increases, recovery of sensory and motor function is often incomplete (Hu, Tian, Prabhakaran, Ding, &

Ramakrishna, 2016; Mcgregor & English, 2019). Autografting is a standard clinical approach to treat regeneration of completely transected nerves. Other approaches include end-to end or end-to-side suturing, allografting, and the use of nerve guide conduits (NGCs; Behbehani et al., 2018; Bell & Haycock, 2012; Grinsell & Keating, 2014; Johnson, Zoubos, & Soucacos, 2005; Pateman et al., 2015). Irrespectively, each of these treatments has limitations and drawbacks that do not support sufficient peripheral nerve regeneration. Research has been conducted to improve the performance

of NGCs, and more recently, focus on the architectural structures within a device to increase trophic support, the addition of neuro-trophic factors, and/or cell therapy (Catrina, Gander, & Madduri, 2013; Madduri, Feldman, Tervoort, Papaloïzos, & Gander, 2010). Neuro-trophic factors support neural regeneration and survival (Madduri, Papaloïzos, & Gander, 2009; Önger et al., 2016), and well-described factors include nerve growth factor (NGF), brain-derived neurotrophic factor (BDNF), glial cell-derived neurotrophic factor (GDNF), and ciliary neurotrophic factor (CNTF; Deister & Schmidt, 2006; Dinis et al., 2015; Fadia et al., 2020; Fine, Decosterd, Papaloïzos, Zurn, & Aebischer, 2002; Madduri et al., 2009). NGF is known to stimulate neurite growth and neural survival after injury (Hu et al., 2016; Zhao et al., 2016), whereas BDNF promotes neuronal survival and morphogenesis (Numakawa et al., 2010). Moreover, GDNF encourages neurite outgrowth and decreases neuronal apoptosis (Fadia et al., 2020; Fine et al., 2002), and CNTF stimulates the remyelination of regenerated neurites (Dinis et al., 2015).

Although neurotrophic factors have previously been introduced into NGCs, nerve repair has not been stimulated significantly, due largely to a short half-life (e.g., 2.3 hr NGF [rat] and 3 hr BDNF [rat]; Kishino et al., 2001; Tria, Fusco, Vantini, & Mariot, 1994), with pro-teolytic degradation and lack of diffusion due to initial single delivery (Lee, Silva, & Mooney, 2011; Tang et al., 2013). Moreover, the re-generation process in large injury gaps (>10 mm) occurs over weeks. Hence, for NGC functionality, it is important to design a sustained delivery system for neurotrophic factors (Achyuta, Cieri, Unger, & Murthy, 2009; Gomez & Schmidt, 2007). Electrochemistry, micro-fluidics, lithography, and microspheres have been used to immobilize neurotrophins in different delivery systems, including NGCs. These techniques can be disadvantageous, because they require complex experimental design and fabrication, leading to long preparation periods, limiting clinical application (Tang et al., 2013) and effec-tiveness on nerve regeneration (Madduri et al., 2010; Moran & Graeber, 2004; Sumner, 1990; Tang et al., 2013). Alternatively, de-velopment of bioactive surfaces in direct contact with regenerating axons will target the delivery of neurotrophic factors more precisely, with direct stimulation for neurite outgrowth.

Biomaterial surfaces are essential for interaction with the en-vironment (Ratner, 2013), and several approaches exist to stimulate biological response (Jones, 2005). Bioactive surfaces as a delivery platform have advantages of controlled, targeted delivery, sustained release, and low dosage. A range of examples are reported, for ex-ample, Puleo, Kissling, and Sheu (2002) immobilized bone morpho-genetic protein onto titanium alloy to promote osteoblastic activity. Ito, Chen, and Imanishi (1998) encouraged fibroblast growth by im-mobilizing epidermal growth factor onto polystyrene.

We have developed a glycosaminoglycan surface platform for growth factor delivery using heparin, through transient charge at-traction of negative functional groups and local release (WO 2017/017425 A1, 2017). For this particular study, we employed a com-mercial source of amine functionalized surfaces that arose directly from this prior study (Robinson et al., 2012). As a method to permit charge attraction, positive surface amine functional groups (NH_2^+)

are created as a basis to attract and bind negatively charged heparin by adsorption to a biomaterial surface of interest (Cao & Li, 2011). We have not previously explored this system for neurotrophin binding and release; however, it is reported that neurotrophins bind to heparin (Casu, Naggi, & Torri, 2015; D. Yang, Moon, & Lee, 2017). The advantage of this method is that it would build the necessary electrostatic positive charge to immobilize neurotrophins, by means of electrostatic interactions between NH_2^+ groups and negatively charged heparin, and by the heparin binding site of neurotrophins. Investigation of a neurotrophin delivery platform is logical to explore for neurite outgrowth by the immobilized of NGFs onto NH_2^+ + heparin surfaces for local and sustained release.

The aim of this study was, therefore, to create experimental bioactive surfaces comprising NH_2^+ and heparin to which im-mobilized NGF, BDNF, or a combination of both could be constructed for release, and neuronal cell response. Herein we report on the design and construction of the system by passive conjugation of heparin and neurotrophic factors. Using primary chick embryo dorsal root ganglion (DRG), enhanced neurite outgrowth was observed when cultured on neurotrophin-enriched surfaces compared to control surfaces tissue culture plastic (TCP), NH_2^+, and NH_2^+ + heparin with soluble growth factors.

2 | MATERIALS AND METHODS

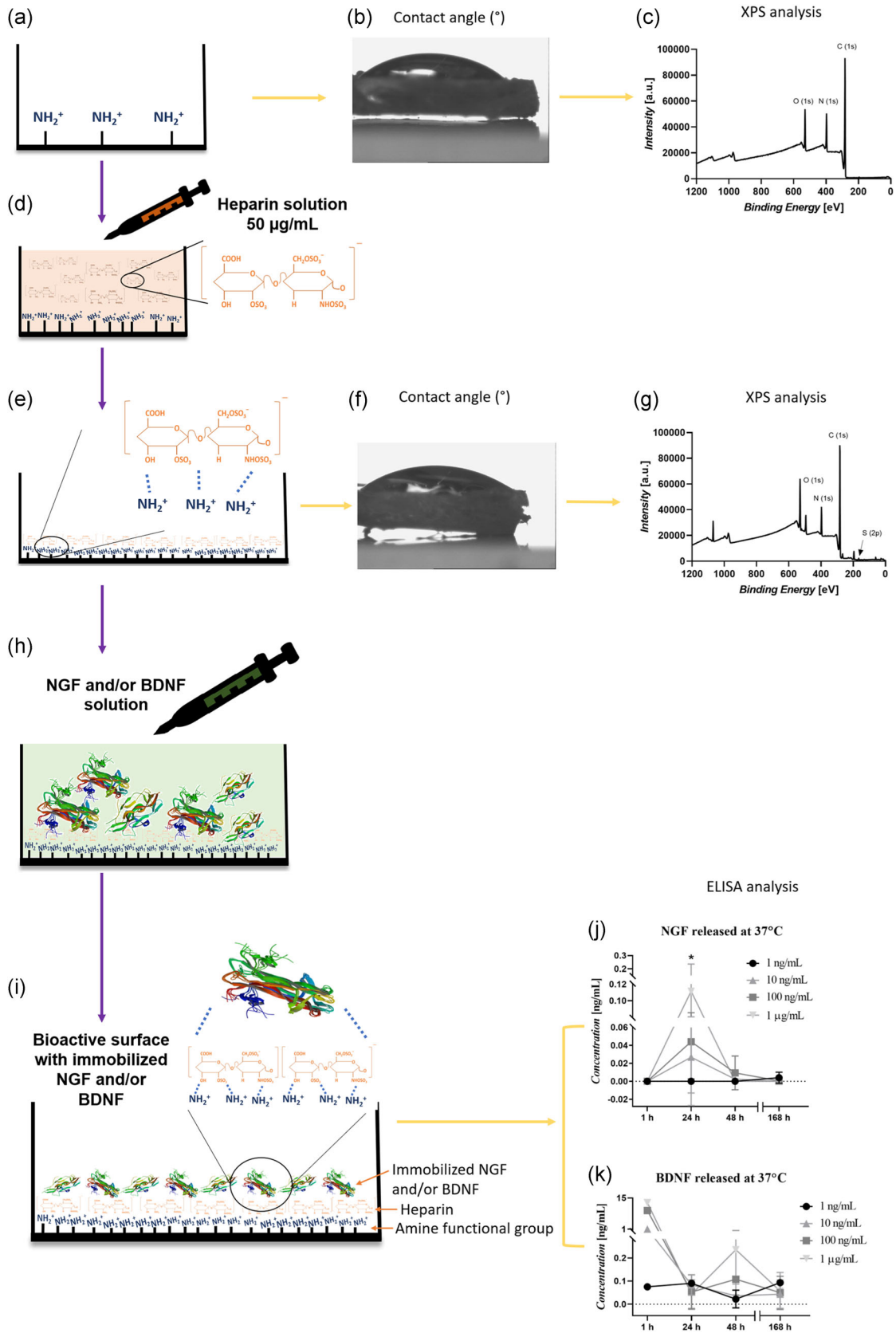### 2.1 | Heparin adsorption to amine functional surfaces

Ninety-six-well plates treated by amine plasma polymerization (Robinson et al., 2012) were sourced (BD PureCoat™; Becton Dickinson, Belgium). A solution of heparin sodium salt from porcine intestinal mucosa (Sigma, UK) was prepared at a concentration of 50 µg/ml. The heparin was ad-ded to the BD PureCoat™ plates and left overnight at room temperature (RT). The heparin solution was then poured off and discarded.

2.2 | Immobilization of NGF and BDNF to amine–heparin surfaces

NGF (R&D Systems), BDNF (R&D Systems), and combinations of the two were immobilized onto the amine–heparin surfaces. Different concentrations of NGF, BDNF, and NGF plus BDNF were prepared at concentrations of 1 pg/ml, 1 ng/ml, 10 ng/ml, 100 ng/ml, and 1 µg/ml. Each solution was added to the amine–heparin surface and incubated for 5 hr at RT, poured off, and discarded. Figure 1 summarizes the design of surfaces immobilized with amine–heparin–neurotrophin.

2.3 | Water contact angle

Water contact angle was measured with a Krüss GmbH drop shape analyzer-100 (DSA100) by placing 5 µl of distilled water on the test

(a)

(b) Contact angle (°)

(c) XPS analysis

(d) Heparin solution 50 µg/mL

(e)

(f) Contact angle (°)

(g) XPS analysis

(h) NGF and/or BDNF solution

(i) Bioactive surface with immobilized NGF and/or BDNF

Immobilized NGF and/or BDNF
Heparin
Amine functional group

ELISA analysis

(j) NGF released at 37°C

1 ng/mL
10 ng/mL
100 ng/mL
1 µg/mL

(k) BDNF released at 37°C

1 ng/mL
10 ng/mL
100 ng/mL
1 µg/mL

surface. The contact angle of surfaces was measured and calculated using DSA100 software.

2.4 | X-ray photoelectron spectroscopy

X-ray photoelectron spectroscopy (XPS) analysis was performed on surfaces at the Sheffield Surface Analysis Centre (The University of Sheffield, UK). Elemental composition (survey scans), nitrogen scans (N1s), and sulfur scans (S2p) were conducted using a Kratos Ultra with a monochromated aluminum source. Elemental survey scans were collected between 0 and 1,200 eV binding energy, and at 160 eV pass energy. N1s and S2p spectra were collected for samples containing amine and heparin, at 20 eV pass energy.

2.5 | Release profile of NGF and BDNF from amine–heparin surfaces

In vitro release of NGF and BDNF was tested by incubating immobilized surfaces with 1 ml of phosphate-buffered saline (PBS) at 37°C. Solution samples were taken at 1, 24, 48, and 168 hr and measured with enzyme-linked immunosorbent assay (ELISA; Yan, Yin, & Li, 2012; Zeng et al., 2014). Briefly, control and test solutions were added to wells and incubated at RT for 2.5 hr, then they were discarded and the plate was rinsed with washing buffer. Biotinylated antibody was added to the wells and incubated for 1 hr at RT. The plate was then rinsed and streptavidin-horseradish peroxidase added for 45 min at RT. 3,3′,5,5′-tetramethylbenzidine substrate was added and incubated for 30 min at RT, followed by stop solution. Absorbance was read at 450 nm using a Bio-Tek ELx 800 microplate reader and KC Junior software.

2.6 | In vitro study using chick embryonic dorsal root ganglia

To evaluate neurotrophin surfaces, embryonic chick DRGs were utilized. Fertilized brown chicken eggs (Henry Stewart & Co. Ltd., UK) were incubated at 37.5°C and 50–70% humidity for 12 days. Embryonic day 12 eggs were opened in a biological safety cabinet to collect the E12 embryo, which was cleaned, and organs were removed (in compliance with UK Home Office Animals [Scientific Procedures] Act 1986 and definition of chicken as a Protected

Animal from E14). DRGs were dissected and under a dissecting microscope, the remains of the root were cut (Powell, Vinod, & Lemons, 2014). DRGs were seeded at a density of one per well on TCP and on bioactive surfaces, with Dulbecco's modified Eagle's medium (DMEM; Sigma) plus 10% (v/v) fetal bovine serum (PAN Biotech, Germany), 1% (w/v) L-glutamine (Sigma), 1% (w/v) penicillin/streptomycin (P/S; Sigma), 0.25% (w/v) amphotericin B (Sigma), and NGF, BDNF, or NGF plus BDNF at the above concentrations. DMEM supplemented with 10% (v/v) fetal calf serum, 1% (w/v) L-glutamine, 1% (w/v) P/S, and 0.25% (w/v) amphotericin was added to samples and DRGs were cultured for 7 days at 37°C and 5% CO_2.

2.7 | Identification of chick DRG neurite growth by βIII-tubulin immunolabelling

Immunolabelling was performed for βIII-tubulin to identify neurons and measure neurite outgrowth. To label cell nuclei, 4′,6-diamidino-2-phenylindole (DAPI, 300 nM; Sigma) was used. Culture medium was discarded from samples and 3.7% (w/v) paraformaldehyde (PFA) was added and incubated for 30 min at RT. PFA was discarded and samples were rinsed three times with PBS (Oxoid, England). Triton X-100 (0.1%; Sigma) with 3% (w/v) bovine serum albumin (BSA; Sigma) in PBS was added and incubated for 1 hr at RT and was then discarded and washed three times. Anti-βIII-tubulin primary antibody (1:1,000; Abcam, UK) in 1% (w/v) BSA/PBS was added and incubated overnight at 4°C, then removed. Alexa Fluor-488 goat anti-mouse secondary antibody (1:400; Life Technologies) in 1% BSA (w/v) in PBS was added to samples and incubated for 3 hr at RT. Samples were then washed three times with PBS. Three hundred nanomole DAPI in PBS was added and incubated for 30 min at RT, then discarded and washed three times with PBS.

2.8 | Epifluorescence microscopy

Whole DRG and neurites were imaged using an inverted Olympus IX73 epifluorescent microscope and Micro-Manager 1.4.22 software (University of California). A mercury lamp was used as the light source. To image βIII-tubulin positive neurites (Alexa Fluor-488) and nuclei (DAPI), excitation and emission wavelengths of $\lambda_{ex} = 488$ nm/$\lambda_{em} = 525$ nm and $\lambda_{ex} = 405$ nm/$\lambda_{em} = 450$ nm were used, respectively. ImageJ 1.52a (National Institutes of Health) was used to measure the length of developed neurites. Neurites were measured from the DRG

FIGURE 1 Design and construction of a biomimetic surface for assisting neuronal growth. (a) NH$_2^+$ surface. (b) Water droplet angle when in contact with NH$_2^+$ surface (43°). (c) X-ray photoelectron spectroscopy (XPS) scan of NH$_2^+$ surface with nitrogen peak visible at 400 eV. (d) Heparin added to NH$_2^+$ surface with electrostatic binding. (e) NH$_2^+$ + heparin surface. (f) Water droplet angle when in contact with NH$_2^+$ + heparin surface (39°). (g) XPS scan of NH$_2^+$ + heparin surface confirming sulfur at 168 eV. (h) Nerve growth factor (NGF) and/or brain-derived neurotrophic factor (BDNF) added to the NH$_2^+$ + heparin surface. (i) Surface immobilized with NGF and/or BDNF. (j) NGF release profile from the loaded surface within 168 hr. (k) BDNF release profile from loaded surface within 168 hr. Adaptation from Paoletti et al. (2016) and Robinson et al. (1999) [Color figure can be viewed at wileyonlinelibrary.com]

to the tip of the neurite. The experiment was repeated three times independently ($N = 3$). Each repeat had three DRGs per condition ($n = 3$). Three images were taken, one per DRG, and 10–15 neurites were measured, per condition, to determine the mean of neurite outgrowth. Background was subtracted (20–30 pixels) to enhance intensity and contrast.
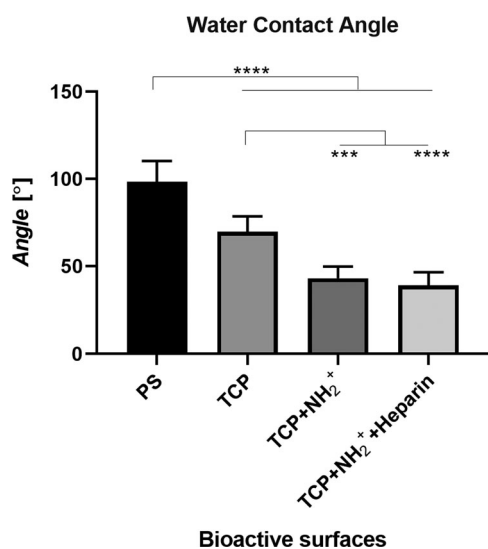
2.9 | Statistical analysis

One-way analysis of variance with a Tukey multiple comparison posttest was performed to identify statistical differences between conditions, using GraphPad Prism 8.2.0. $p < .05$ was considered significant.

3 | RESULTS

3.1 | Characterization of surfaces by water contact angle

Water contact angles were measured by sessile drop as a measure of relative hydrophilicity (Liu et al., 2014). The mean contact angles of polystyrene (PS), TCP, TCP + NH_2^+, and TCP + NH_2^+ + heparin were 98, 70, 43, and 39°, respectively (Figure 2). The decrease in the contact angle confirmed the presence of charged functional groups at the surface, such as amine (NH_2^+) and sulfate. The lowest contact angle was observed for TCP + NH_2^+ + heparin. PS control angles were significantly different compared to TCP + NH_2^+ and TCP + NH_2^+ +

heparin surfaces (****$p < .0001$). TCP angles were also significantly different when compared with TCP + NH_2^+ and TCP + NH_2^+ + heparin surfaces (***$p < .001$ and ****$p < .0001$, respectively). There was no difference between the contact angles for TCP + NH_2^+ and TCP + NH_2^+ + heparin.

3.2 | Characterization surfaces by XPS

XPS analysis was used to determine elemental composition of surfaces after each modification step. Chemical survey scans of each are shown in Figure 1. TCP + NH_2^+ surfaces and TCP + NH_2^+ + heparin surfaces identified a peak at 400 eV, confirming the presence of nitrogen with 12.6% and 9.15% of atomic composition (Figure 1c and 1g and Figure S1A). Furthermore, N1s scan revealed a single peak, which was attributed to the NH_2^+ content on the TCP + NH_2^+ surface and TCP + NH_2^+ + heparin surface (Figure S1B and S1C), as TCP has a negligible nitrogen content (Koller, Palsson, Manchel, Maher, & Palsson, 1998). Moreover, the decreased nitrogen content in the TCP + NH_2^+ + heparin surface could possibly be due to the loss of nitrogen after the incubation step of heparin, during the rinsing step (Dehili, Lee, Shakesheff, & Alexander, 2006). An S2p peak was detected for the TCP + NH_2^+ + heparin surface at 168 eV (Figure 1g). Figure S1D shows the S2p scan with S2p$^{3/2}$ and S2p$^{1/2}$. This confirmed the presence of sulfur, and hence heparin.

3.3 | Release of NGF and BDNF from NH_2^+ + heparin surfaces

NGF release from NH_2^+ + heparin surfaces was measured over 168 hr by ELISA (Figure 1j and Table 1). None of the surfaces immobilized with NGF, at any of the used concentrations, released NGF within 1 hr. For surfaces immobilized with NGF at 1 µg/ml, 0.03% of the total dose was detected at 24 hr. For surfaces immobilized with NGF at 100 ng/ml, 1% (24 hr) and 0.04% (48 hr) were detected, respectively. NGF release was quantified at 24 and 48 hr for surfaces immobilized with 10 ng/ml, with 1% and 0.06% of total load detected, respectively. Surfaces immobilized with NGF at the lower concentration of 1 ng/ml did not show growth factor release at 24 or 48 hr; however, at 168 hr, 1% of NGF was detected. Quantification of BDNF released from surfaces was evaluated over 168 hr by ELISA (Figure 1k and Table 1). For surfaces immobilized with BDNF at 1 µg/ml, 3% and 0.01% of the total dose was measured at 1 and 24 hr. Moreover, 0.06% and 0.01% was measured after 48 and 168 hr, respectively. For surfaces immobilized with BDNF at 100 ng/ml, 32% (1 hr), 0.18% (24 hr), 0.37% (48 hr), and 0.17% (168 hr) of initial load was detected, respectively. BDNF was quantified at 1, 24, 48, and 168 hr for surfaces immobilized with 10 ng/ml, resulting in 35%, 2.8%, 1.2%, and 1.5% of initial load, respectively. Surfaces immobilized with BDNF at 1 ng/ml showed 25%, 30%, 11%, and 31% of growth factor release at 1, 24, 48, and 168 hr.

Water Contact Angle

FIGURE 2 Water contact angle for each surface (±SD). Polystyrene (98°), tissue culture polystyrene (TCP; 70°), TCP + NH_2^+ (TCP + amine functionalized surface; 43°), and TCP + NH_2^+ + heparin; 39°) surfaces. ($N = 3$ and $n = 3$). One-way analysis of variance (ANOVA) with Tukey multiple comparison test was performed. ****$p < .0001$ and ***$p < .001$

TABLE 1 Released concentration of NGF or BDNF from the bioactive surface at 1, 24, 48, and 168 hr

		Released concentration (ng/ml) from bioactive surface/released percentage (%) from the total immobilized load							
		1 ng/ml		10 ng/ml		100 ng/ml		1 µg/ml	
		ng/ml	%	ng/ml	%	ng/ml	%	ng/ml	%
NGF	1 hr	0 ± 0	0	0 ± 0	0	0 ± 0	0	0 ± 0	0
	24 hr	0 ± 0	0	0.027 ± 0.054	1	0.044 ± 0.041	1	0.115 ± 0.146	0.03
	48 hr	0 ± 0	0	0.002 ± 0.002	0.06	0.009 ± 0.019	0.04	0 ± 0	0
	168 hr	0.004 ± 0.004	1	0 ± 0	0	0 ± 0	0	0 ± 0	0
BDNF	1 hr	0.075 ± 0	25	1.04 ± 0	35	9.35 ± 0	32	12.92 ± 0	3
	24 hr	0.090 ± 0.008	30	0.083 ± 0.043	2.8	0.053 ± 0.074	0.18	0.043 ± 0.06	0.01
	48 hr	0.033 ± 0.047	11	0.036 ± 0.050	1.2	0.108 ± 0.013	0.37	0.243 ± 0.18	0.06
	168 hr	0.096 ± 0.003	31	0.043 ± 0.061	1.5	0.05 ± 0.071	0.17	0.049 ± 0.07	0.01

Note: This concentration is also presented as a percentage calculated from the initial immobilized neurotrophin load.
Abbreviations: BDNF, brain-derived neurotrophic factor; NGF, nerve growth factor.

3.4 | Chick dorsal root ganglion neurite outgrowth

Normal chick primary DRGs were cultured on surfaces immobilized with concentrations of NGF, BDNF, and NGF + BDNF from 1 pg/ml to 1 µg/ml. Figure 3 shows average neurite length developed by the DRGs after 7 days in culture. Neurite outgrowth was significantly increased for DRGs grown on surfaces immobilized with NGF at 1 ng/ml, in comparison with control surfaces of TCP, NH_2^+ alone, and NH_2^+ + heparin alone. Moreover, neurite outgrowth from surfaces immobilized with NGF, BDNF, and NGF plus BDNF were longer than neurites developed on the control surfaces of TCP, NH_2^+ alone, and NH_2^+ + heparin alone (Figure 3d). As seen in Figure 3a, DRG neurites were longest when grown on surfaces immobilized with NGF at 1 ng/ml. Neurite lengths were less when grown on NGF surfaces of 10 ng/ml and 1 µg/ml. A similar response was observed for neurite outgrowth with immobilized BDNF (Figure 3b). Longest neurite development was observed when DRGs were cultured on BDNF surfaces at 1 ng/ml. When DRGs were cultured on surfaces immobilized with NGF plus BDNF (Figure 3c), neurite outgrowth was longest for 100-ng/ml surfaces. These results demonstrate that immobilizing neurotrophic factors either as NGF, BDNF, or a combination of both can support neurite growth. Immobilized NGF had a more positive effect, compared to immobilized BDNF. Immobilization of NGF plus BDNF did not have an additive effect compared to either neurotrophin alone on neurite length (except at 1 pg/ml).

4 | DISCUSSION

NGF and BDNF were immobilized at different concentrations on surfaces comprising NH_2^+ + heparin to form a biomaterial substrate optimal for enhancing neurite outgrowth. Culture of primary chick DRGs isolated at E12 were used to evaluate neurotrophin functionalized surfaces. Studies have previously investigated NGF, BDNF, and GDNF in conjunction with scaffolds and nerve guide tubes, and evaluated neurite expression (Achyuta et al., 2009; Gomez &

Schmidt, 2007; Kapur & Shoichet, 2004; Madduri et al., 2010; Santos, Gonzalez-Perez, Navarro, & Del Valle, 2016; Tang et al., 2013). In these studies, neurotrophins were associated with biomaterial surfaces using different approaches. Interestingly, the concentration of neurotrophin required was higher than those used in the present study. Gomez and Schmidt (2007) immobilized NGF at 1 ng/mm^2 on polypyrrole by a photochemical technique with average neurite lengths of 20 µm after 2 days of rat DRG culture. Tang et al. (2013) used a silk fibroin coating to immobilize NGF as a gradient on poly(ε-caprolactone)-poly(L-lactic) acid. The cumulative release of NGF ranged from 3.6 to 11.35 ng/ml within 7 days. Neurite lengths of DRGs after 3 days in culture varied according to the gradient zone, from 600 to 1,500 µm (Tang et al., 2013). In contrast, surfaces created herein formed a platform to deliver immobilized neurotrophins after 7 days release using less than 1 ng/ml from 1 to 168 hr. Maximum average neurite length of 1,075 µm was observed when surfaces were immobilized with NGF at 1 ng/ml. This suggests that neurotrophin delivery is more efficient by using growth factors at less than 1 ng/ml for stimulating neurite lengths greater than 1,000 µm in vitro.

Evidence in support of functional surface characterization included water contact angle, initially conducted to evaluate relative wettability of the modified material. Surface wettability will change due to the presence of positively charged amine groups (Li, Li, Yu, & Sun, 2017) or negatively charged heparin (Cao & Li, 2011; Mascotti & Lohman, 1995; T. Yang et al., 2006). Results showed a decrease in contact angle, leading to an increase in hydrophilicity. Changes in contact angle and relative wettability of modified surfaces ranged from 70° (TCP), 43° (TCP + NH_2^+) to 39° (TCP + NH_2^+ + heparin) provided evidence of surface modification. Addition of amine groups and heparin demonstrated the relative hydrophilicity for each modification, where TCP + NH_2^+ surfaces and TCP + NH_2^+ + heparin surfaces were the most hydrophilic. These data are supported by Zhou and Meyerhoff (2005), Liu et al. (2014), and Smith et al. (2016), where contact angle decreases are reported for amine group and heparin surface modification, respectively.
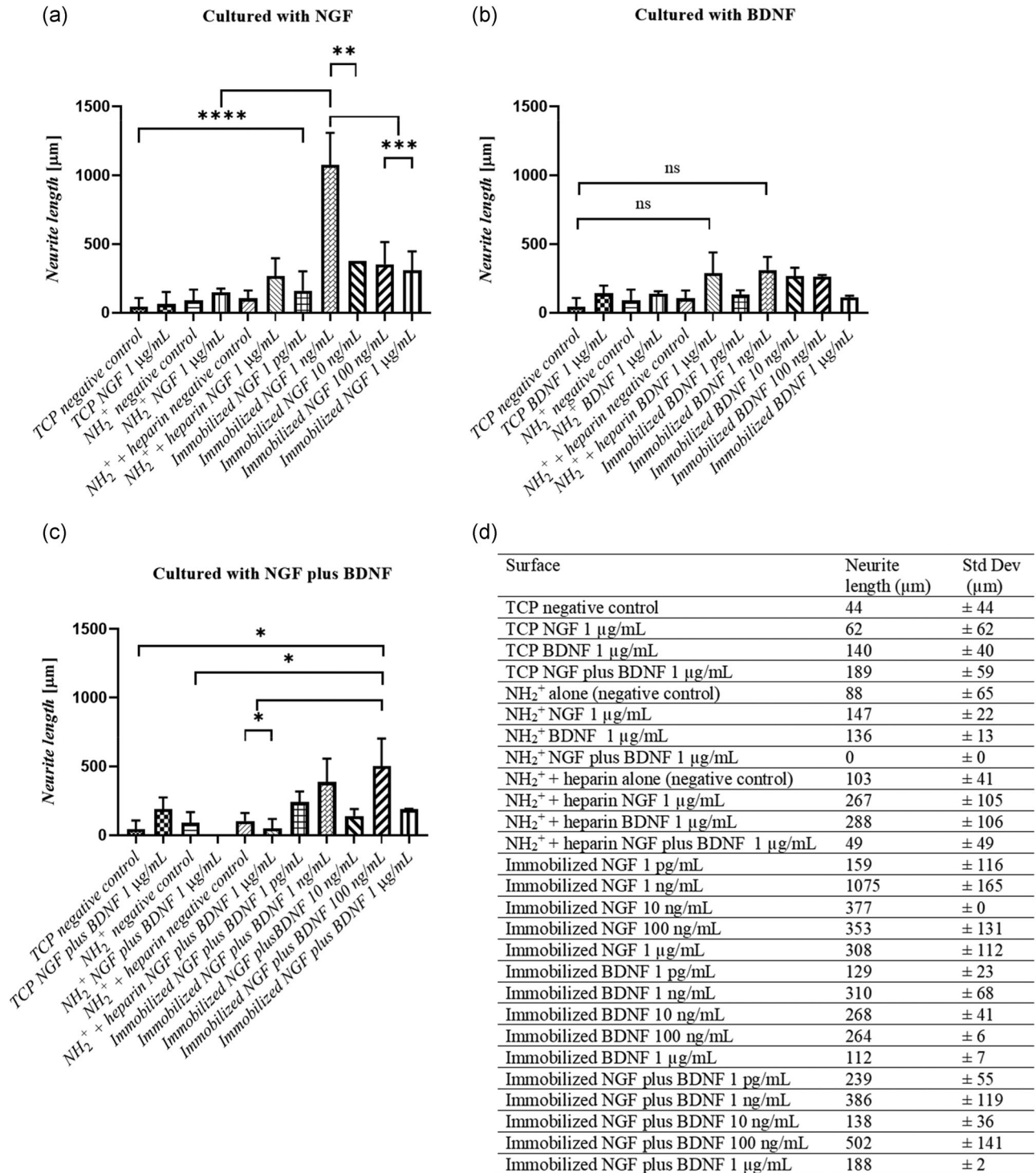
FIGURE 3 Average neurite length grown over 7 days by chick embryo dorsal root ganglion (DRGs; E12) on TCP, NH_2^+, and NH_2^+ + heparin surfaces in the presence of soluble (control) and immobilized surfaces (test) (a) cultured with NGF, (b) cultured with BDNF, and (c) cultured with NGF plus BDNF. Bars = ±SD. (d) Average neurite length values. Three experiments were performed independently; three DRGs were seeded per condition ($N = 3$ and $n = 3$). One-way ANOVA with Tukey multiple comparison test was performed (*$p < .05$, **$p < .01$, ***$p < .001$, and ****$p < .0001$). ANOVA, analysis of variance; BDNF, brain-derived neurotrophic factor; NGF, nerve growth factor; TCP, tissue culture polystyrene

We hypothesized that heparin binds electrostatically to surface amine groups through attractive electrostatic force and have developed a glycosaminoglycan surface platform for growth factor delivery using heparin, through transient charge attraction of negative functional groups and local release (WO 2017/017425 A1, 2017). For this particular study, we employed a commercial BD PureCoat™ source of amine functional surfaces that arose from a prior study (Robinson et al., 2012). This study precedes and underpins the application reported herein. The amine coated plates were used to fabricate the heparin + neurotrophin layers. This was the first step to study the effectiveness of this delivery platform on neurite outgrowth. XPS analysis confirmed the presence of amine groups, and separately the presence of sulfur for heparin at the modified surface. This was paramount because to scale and apply this bioactive surface to other biomaterials, we need to replicate the nitrogen content on the commercially amine coated plates to replicate the results presented in this study. Therefore, we will aim to incorporate NH_2^+ groups by plasma polymerization, as this process has effectively deposited amine groups in different materials (Beck et al., 2005; Dehili et al., 2006; Smith et al., 2016). The formation of an NH_2^+ + heparin surface was used as a basis to permit NGF and BDNF immobilization in the heparin layer, and a platform the study of enhanced neurite outgrowth when in direct contact.

Studies have previously reported on chemically binding heparin to coatings and scaffolds (Kim, Kang, Huh, & Yoon, 2000; Liu et al., 2014; Zhou & Meyerhoff, 2005). Gigliobianco, Chong, and Macneil (2015) bound heparin to alternate layers of polyethyleneimine (positively charged) and heparin or polyethyleneimine and polyacrylic acid by repeated rounds of electrostatic adsorption using acrylic acid plasma deposition (known to have negatively charged carboxyl groups; Campbell & Farrel, 2008). Their results showed that heparin bound to alternate layers of polyethyleneimine and acrylic acid. Moreover, heparin bound to positively charged polyethyleneimine after seven layers of coating, whereas no heparin was bound after five layers of coating (Gigliobianco et al., 2015). This finding raises the question as to whether heparin could bind to other positively charge functional groups, such as NH_2^+. The atomic percentage of sulfur (found in heparin) present in seven layers of polyethyleneimine was 0.53% (Gigliobianco et al., 2015). In comparison, the present study demonstrated an atomic percentage of 0.69% for sulfur on TCP + NH_2^+ + heparin surfaces. This supported the hypothesis that heparin was bound to the positively charged amine groups at the surface.

Heparin is also known to bind growth factors (Meneghetti et al., 2015; Sakiyama-Elbert & Hubbell, 2000), including NGF and BDNF (Sakiyama-Elbert & Hubbell, 2000), albeit with moderate affinity. Considering these studies, we hypothesized that NGF and BDNF would bind sufficiently through electrostatic and noncovalent interactions, and with overall surface energy to immobilize. ELISA analysis for each neurotrophin was used to investigate if the growth factors were eluted over a timeframe consistent with nerve cell interaction and growth at 1, 24, 48, and 168 hr. Results showed that for each time point, the release was <35% of the total growth factor

immobilized onto the surface. Interestingly, surfaces immobilized with NGF at 1 ng/ml did not show any release until Day 7 (168 hr). This kinetic profile was of note and was hypothesized as advantageous in regard to neural implant applications for repair, mapping broadly to the initial stages of nerve repair following injury.

According to Roach, Eglin, Rohde, and Perry (2007), after implantation of a biomaterial, water molecules form an intimate layer. Proteins then adsorb on the material surface, and adherent cells that express functionally binding integrins reach the surface and start to interact with the protein layer. Thereafter, cells adhere, migrate, and differentiate. This last step occurs from a few hours to a few days after implantation. As functionalized surfaces containing immobilized NGF at 1 ng/ml did not show any growth factor release between 1 and 48 hr, therefore, such a delivery platform could permit time for neuronal cells to adhere to a regenerating guidance scaffold surface before receiving stimuli from NGF at the surface to stimulate growth.

Chick embryo DRGs were cultured on surfaces containing immobilized neurotrophins. Neurite development is shown in Figure 4. DRGs were used for their accessibility and are comparable with other model animal systems in regard to neurite regeneration (Kuhn, Stoeckli, Condrau, Rathjen, & Sonderegger, 1991; Stoeckli et al., 1989; Stoeckli, Kuhn, Duc, Ruegg, & Sonderegger, 1991). Surfaces with immobilized NGF at 1 ng/ml stimulated longest growth of neurite in all groups. Neurite outgrowth was 18 times higher for immobilized NGF (1 ng/ml) surfaces than negative TCP control surfaces. The response of DRGs on immobilized BDNF surfaces demonstrated a similar response, compared to immobilized NGF surfaces, with 1-ng/ml surfaces showing the largest response. Surfaces immobilized with NGF + BDNF at 100 ng/ml supported DRG neurite lengths significantly longer than those on TCP negative control surfaces, or TCP containing NGF at 1 μg/ml.

The different response of neurite outgrowth can be hypothesized through activated second message pathways, following growth factor binding to cell surface expressed membrane receptors. Both NGF and BDNF bind to the tyrosine kinase receptors (Trk), TrkA and TrkB, respectively (Madduri et al., 2009; Santos et al., 2016). NGF–TrkA complexes are internalized at the neurite growth cones and retrogradely transported to the soma, inducing microtubule and actin polymerization, calcium influx, and organelle recruitment (Kapur & Shoichet, 2004). However, when NGF–TrkA complexes are not internalized, activation of the phosphatidylinositol 3-kinase and Akt/protein kinase B (PI3K/Akt) pathways arise, which regulate cell survival and neurite extension (Gomez & Schmidt, 2007; Madduri et al., 2009; Tang et al., 2013). When BDNF binds to TrkB receptors, the PI3K/Akt pathway is triggered and microtubules are rearranged to encourage filopodial elongation and lamellipodial formation (Mcgregor & English, 2019). Hence, Trk receptors activate signaling pathways which encourage neurite elongation in sensory and motor neurons.

In DRGs, TrkA and TrkB receptors are expressed in the cell membrane. However, the density of TrkB receptors is lower compared to TrkA receptors (McMahon, Armanini, Ling, & Phillips, 1994). Nevertheless, the expression of TrkB receptors is upregulated after
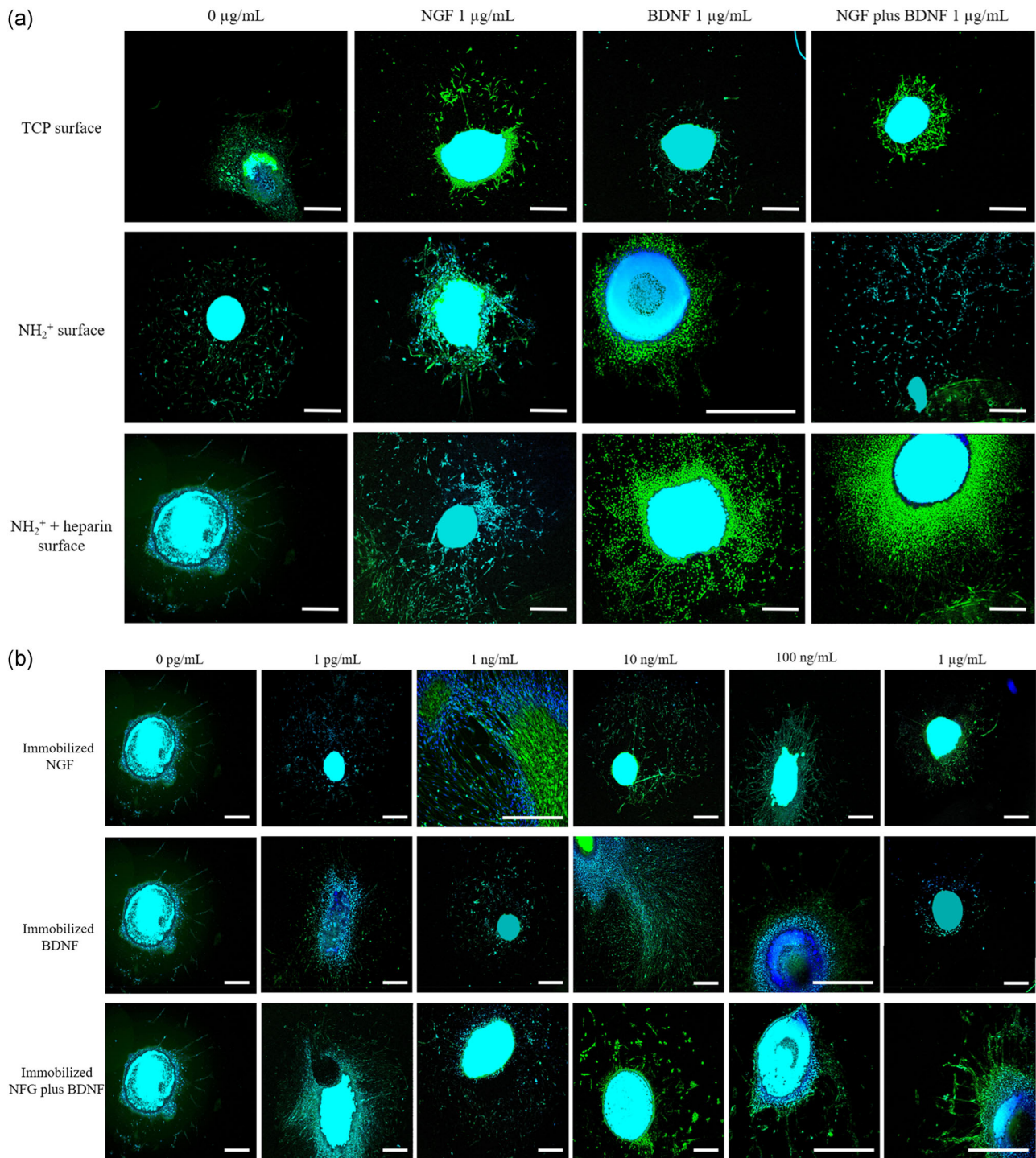
FIGURE 4 Primary chick DRGs cultured on (a) Control, TCP, NH_2^+, and NH_2^+ + heparin in the presence of soluble NGF, BDNF, or NGF plus BDNF. (b) Surfaces immobilized with NGF, BDNF, or NGF plus BDNF at different concentrations. β-III-tubulin is labeled in green. Nuclei are labeled in blue. Scale bar = 500 μm. BDNF, brain-derived neurotrophic factor; DRG, dorsal root ganglion; NGF, nerve growth factor; TCP, tissue culture polystyrene [Color figure can be viewed at wileyonlinelibrary.com]

injury (Santos et al., 2016). Hence, both NGF and BDNF are needed to prevent cell death and to stimulate neurite outgrowth. The present data would suggest that TrkB receptor expression is low, because neurite growth on immobilized BDNF surface was similar to NGF immobilized surfaces. When NGF and BDNF were coimmobilized, neurite length was not cumulative. This effect could be related to the concentration of BDNF released from the surface, since low doses of BDNF upregulate the expression of TrkB receptors, maximizing the effect of BDNF. In contrast, high doses would be expected to downregulate the density of TrkB receptors.

Moreover, high doses of BDNF would inhibit neurite elongation (Santos et al., 2016), whereas low doses of BDNF stimulate neurite outgrowth in sensory neurons (e.g., DRGs). Thus, when delivered with NGF, an equilibrium would be expected.

In summary, we report on the design, manufacture, physico-chemical and biological characterization of surfaces immobilized with NGF and BDNF using commercially amine coated plates and heparin. NGF loaded surfaces at 1 ng/ml encouraged longest neurite lengths due to (a) DRGs having sufficient time to attach to surfaces and (b) neurotrophin release being controlled over a similar timeframe. DRG neurites most likely formed via activation of PI3K through membrane activation of NGF–TrkA. The system reported is relatively simple to produce, and scalable for direct applications, using plasma poly-merization, for enhancing the function of NGCs to enhance nerve growth following acute injury.

5 | CONCLUSION

This study reports on the design and construction of bioactive sur-faces with heparin bound electrostatically to amine groups, that can be used to immobilize NGF and BDNF. The surface was used as a model platform for delivery of NGF and BDNF. Bioactive surfaces stimulated neurite outgrowth in DRGs using very low concentrations of neurotrophin, making this approach directly applicable and scal-able for improving the function of existing NGCs.

ACKNOWLEDGMENTS

ORCID

John W. Haycock ￼ http://orcid.org/0000-0002-3950-3583

REFERENCES

Achyuta, A. K. H., Cieri, R., Unger, K., & Murthy, S. K. (2009). Synergistic effect of immobilized laminin and nerve growth factor on PC12 neurite outgrowth. *Biotechnology Progress*, 25(1), 227–234. https://doi.org/10.1002/btpr.58

Behbehani, M., Glen, A., Taylor, C. S., Schuhmacher, A., Claeyssens, F., & Haycock, J. W. (2018). Pre-clinical evaluation of advanced nerve guide conduits using a novel 3D in vitro testing model. *International Journal of Bioprinting*, 4(1). https://doi.org/10.18063/ijb.v4i1.123

Beck, A. J., Whittle, J. D., Bullett, N. A., Eves, P., Mac Neil, S., McArthur, S. L., & Shard, A. G. (2005). Plasma co-polymerisation of two strongly interacting monomers: Acrylic acid and allylamine. *Plasma Processes and Polymers*, 2(8), 641–649. https://doi.org/10.1002/ppap.200500043

Bell, J. H. A., & Haycock, J. W. (2012). Next generation nerve guides: Materials, fabrication, growth factors, and cell delivery. *Tissue Engineering Part B: Reviews*, 18(2), 116–128. https://doi.org/10.1089/ten.teb.2011.0498

Campbell, M. K., & Farrell, S. O. (2008). Amino acids and peptides, *Biochemistry* (6th ed, pp. 73–76). Belmont, CA: Thomson/Brooks/Cole.

Cao, R., & Li, B. (2011). A simple and sensitive method for visual detection of heparin using positively-charged gold nanoparticles as colorimetric probes. *Chemical Communications*, 47, 2865–2867. https://doi.org/10.1039/c0cc05094f

Casu, B., Naggi, A., & Torri, G. (2015). Re-visiting the structure of heparin. *Carbohydrate Research*, 403, 60–68. https://doi.org/10.1016/j.carres.2014.06.023

Catrina, S., Gander, B., & Madduri, S. (2013). Nerve conduit scaffolds for discrete delivery of two neurotrophic factors. *European Journal of Pharmaceutics and Biopharmaceutics*, 85(1), 139–142. https://doi.org/10.1016/j.ejpb.2013.03.030

Crawford-Corrie, A., Buttle, D. J., & Haycock, J. W. (2017). *WO 2017/017425 A1*. The University of Sheffield: Great Britain.

Daly, W., Yao, L., Zeugolis, D., Windebank, A., & Pandit, A. (2012). A biomaterials approach to peripheral nerve regeneration: Bridging the peripheral nerve gap and enhancing functional recovery. *Journal of the Royal Society Interface*, 9, 202–221. https://doi.org/10.1098/rsif.2011.0438

Dehili, C., Lee, P., Shakesheff, K. M., & Alexander, M. R. (2006). Comparison of primary rat hepatocyte attachment to collagen and plasma-polymerised allylamine on glass. *Plasma Processes and Polymers*, 3(6–7), 474–484. https://doi.org/10.1002/ppap.200500169

Deister, C., & Schmidt, C. E. (2006). Optimizing neurotrophic factor combinations for neurite outgrowth. *Journal of neural engineering*, 3(2), 172–179. https://doi.org/10.1088/1741-2560/3/2/011

Dinis, T. M., Elia, R., Vidal, G., Dermigny, Q., Denoeud, C., Kaplan, D. L., … Marin, F. (2015). 3D multi-channel bi-functionalized silk electrospun conduits for peripheral nerve regeneration. *Journal of the Mechanical Behavior of Biomedical Materials*, 41, 43–55. https://doi.org/10.1016/j.jmbbm.2014.09.029

Fadia, N. B., Bliley, J. M., DiBernardo, G. A., Crammond, D. J., Schilling, B. K., Sivak, W. N., … Marra, K. G. (2020). Long-gap peripheral nerve repair through sustained release of a neurotrophic factor in nonhuman primates. *Science Translational Medicine*, 12(527), https://doi.org/10.1126/scitranslmed.aav7753

Fine, E. G., Decosterd, I., Papaloïzos, M., Zurn, A. D., & Aebischer, P. (2002). GDNF and NGF released by synthetic guidance channels support sciatic nerve regeneration across a long gap. *European Journal of Neuroscience*, 15, 589–601. https://doi.org/10.1046/j.1460-9568.2002.01892.x

Gigliobianco, G., Chong, C. K., & Macneil, S. (2015). Simple surface coating of electrospun poly-L-lactic acid scaffolds to induce angiogenesis. *Journal of Biomaterials Applications*, 30(1), 50–60. https://doi.org/10.1177/0885328215569891

Gomez, N., & Schmidt, C. E. (2007). Nerve growth factor-immobilized polypyrrole: Bioactive electrically conducting polymer for enhanced neurite extension. *Journal of Biomedical Materials Research - Part A*, 81A, 135–149. https://doi.org/10.1002/jbm.a.31047

Grinsell, D., & Keating, C. P. (2014). Peripheral nerve reconstruction after injury: A review of clinical and experimental therapies. *BioMed Research International*, 2014. https://doi.org/10.1155/2014/698256

Hu, J., Tian, L., Prabhakaran, M. P., Ding, X., & Ramakrishna, S. (2016). Fabrication of nerve growth factor encapsulated aligned poly(ε-caprolactone) nanofibers and their assessment as a potential neural tissue engineering scaffold. *Polymers*, 8(54), https://doi.org/10.3390/polym8020054

Hughes, R. (2008). Peripheral nerve diseases. *Practical Neurology*, 8, 396–405. https://doi.org/10.1136/jnnp.2008.162412

Ito, Y., Chen, G., & Imanishi, Y. (1998). Micropatterned immobilization of epidermal growth factor to regulate cell function. *Bioconjugate Chemistry*, 9(2), 277–282. https://doi.org/10.1021/bc970190b

Johnson, E. O., Zoubos, A. B., & Soucacos, P. N. (2005). Regeneration and repair of peripheral nerves. *Injury, International Journal of the Care of the Injured*, 365, S24–S29. https://doi.org/10.1016/j.injury.2005.10.012

Jones, J. R. (2005). Scaffolds for tissue engineering. In J. R. Hench, L. Larry & Jones (Eds.), *Biomaterials, Artificial Organs and Tissue Engineering* (pp. 201–214). Cambridge, UK: Woodhead Publishing.

Kapur, T. A., & Shoichet, M. S. (2004). Immobilized concentration gradients of nerve growth factor guide neurite outgrowth. *Journal of Biomedical Materials Research - Part A*, 68(2), 235–243. https://doi.org/10.1002/jbm.a.10168

Kim, Y. J., Kang, I. K., Huh, W., & Yoon, S. C. (2000). Surface characterization and in vitro blood compatibility of poly(ethylene terephthalate) immobilized with insulin and/or heparin using plasma glow discharge. *Biomaterials*, 21, 121–130.

Kishino, A., Katayama, N., Ishige, Y., Yamamoto, Y., Ogo, H., Tatsuno, T., ... Nakayama, C. (2001). Analysis of effects and pharmacokinetics of subcutaneously administered BDNF. *Neuroreport*, 12(5), 1067–1072. https://doi.org/10.1097/00001756-200104170-00040

Koller, M. R., Palsson, M. A., Manchel, I., Maher, R. J., & Palsson, B. (1998). Tissue culture surface characteristics influence the expansion of human bone marrow cells. *Biomaterials*, 19(21), 1963–1972. https://doi.org/10.1016/S0142-9612(98)00101-X

Kuhn, T. B., Stoeckli, E. T., Condrau, M. A., Rathjen, F. G., & Sonderegger, P. (1991). Neurite outgrowth on immobilized axonin-1 is mediated by a heterophilic interaction with L1(G4). *Journal of Cell Biology*, 115(4), 1113–1126. https://doi.org/10.1083/jcb.115.4.1113

Lee, K., Silva, E. A., & Mooney, D. J. (2011). Growth factor delivery-based tissue engineering: General approaches and a review of recent developments. *Journal of the Royal Society Interface*, 8, 153–170. https://doi.org/10.1098/rsif.2010.0223

Li, M., Li, Y., Yu, L., & Sun, Y. (2017). Characterization of poly(allylamine) as a polymeric ligand for ion-exchange protein chromatography. *Journal of Chromatography A*, 1486, 103–109. https://doi.org/10.1016/j.chroma.2016.11.012

Liu, T., Liu, Y., Chen, Y., Liu, S., Maitz, M. F., Wang, X., ... Huang, N. (2014). Immobilization of heparin/poly-L-lysine nanoparticles on dopamine-coated surface to create a heparin density gradient for selective direction of platelet and vascular cells behavior. *Acta Biomaterialia*, 10(5), 1940–1954. https://doi.org/10.1016/j.actbio.2013.12.013

Lundborg, G. (2003). Nerve injury and repair – a challenge to the plastic brain. *Journal of the Peripheral Nervous system*, 8(4), 209–226. https://doi.org/10.1111/j.1085-9489.2003.03027.x

Madduri, S., Feldman, K., Tervoort, T., Papaloïzos, M., & Gander, B. (2010). Collagen nerve conduits releasing the neurotrophic factors GDNF and NGF. *Journal of Controlled Release*, 143(2), 168–174. https://doi.org/10.1016/j.jconrel.2009.12.017

Madduri, S., Papaloïzos, M., & Gander, B. (2009). Synergistic effect of GDNF and NGF on axonal branching and elongation in vitro. *Neuroscience Research*, 65(1), 88–97. https://doi.org/10.1016/j.neures.2009.06.003

Mascotti, D. P., & Lohman, T. M. (1995). Thermodynamics of charged oligopeptide-heparin Interactions. *Biochemistry*, 34(9), 2908–2915. https://doi.org/10.1021/bi00009a022

Mcgregor, C. E., & English, A. W. (2019). The role of BDNF in peripheral nerve regeneration: Activity-dependent treatments and Val66Met. *Frontiers in Cellular Neuroscience*, 12(522), https://doi.org/10.3389/fncel.2018.00522

McMahon, S. B., Armanini, M. P., Ling, L. H., & Phillips, H. S. (1994). Expression and coexpression of Trk receptors in subpopulations of adult primary sensory neurons projecting to identified peripheral targets. *Neuron*, 12(5), 1161–1171. https://doi.org/10.1016/0896-6273(94)90323-9

Meneghetti, M. C. Z., Hughes, A. J., Rudd, T. R., Nader, H. B., Powell, A. K., Yates, E. A., & Lima, M. A. (2015). Heparan sulfate and heparin interactions with proteins. *Journal of the Royal Society Interface*, 12. https://doi.org/10.1098/rsif.2015.0589

Moran, L. B., & Graeber, M. B. (2004). The facial nerve axotomy model. *Brain Research Reviews*, 44, 154–178. https://doi.org/10.1016/j.brainresrev.2003.11.004

Numakawa, T., Suzuki, S., Kumamaru, E., Adachi, N., Richards, M., & Kunugi, H. (2010). BDNF function and intracellular signaling in neurons. *Histology and Histopathology*, 25, 237–258.

Önger, M. E., Delibaş, B., Türkmen, A. P., Erener, E., Altunkaynak, B. Z., & Kaplan, S. (2016). The role of growth factors in nerve regeneration. *Drug Discoveries & Therapeutics*, 10(6), 285–291. https://doi.org/10.5582/ddt.2016.01058

Paoletti, F., de Chiara, C., Kelly, G., Covaceuszach, S., Malerba, F., Yan, R., ... Pastore, A. (2016). Conformational rigidity within plasticity promotes differential target recognition of nerve growth factor. *Frontiers in Molecular Biosciences*, 3, 83.

Pateman, C. J., Harding, A. J., Glen, A., Taylor, C. S., Christmas, C. R., Robinson, P. P., ... Haycock, J. W. (2015). Nerve guides manufactured from photocurable polymers to aid peripheral nerve repair. *Biomaterials*, 49, 77–89. https://doi.org/10.1016/j.biomaterials.2015.01.055

Powell, S., Vinod, A., & Lemons, M. L. (2014). Isolation and culture of dissociated sensory neurons from chick embryos. *Journal of Visualized Experiments*, 91, 1–8. https://doi.org/10.3791/51991

Puleo, D. A., Kissling, R. A., & Sheu, M. (2002). A technique to immobilize bioactive proteins, including bone morphogenetic protein-4 (BMP-4), on titanium alloy. *Biomaterials*, 23, 2079–2087.

Ratner, B. D. (2013). Surface properties and surface characterization of biomaterials. In B. D. Ratner, A. S. Hoffman, F. J. Schoen & J. E. Lemons (Eds.), *Biomaterials Science. An Introduction to Materials in Medicine* (3rd ed, pp. 34–53). Oxford, UK: Academic Press.

Roach, P., Eglin, D., Rohde, K., & Perry, C. C. (2007). Modern biomaterials: A review—bulk properties and implications of surface modifications. *Journal of Materials Science: Materials in Medicine*, 18, 1263–1277. https://doi.org/10.1007/s10856-006-0064-3

Robinson, D. E., Buttle, D. J., Short, R. D., McArthur, S. L., Steele, D. A., & Whittle, J. D. (2012). Glycosaminoglycan (GAG) binding surfaces for characterizing GAG-protein interactions. *Biomaterials*, 33(4), 1007–1016. https://doi.org/10.1016/j.biomaterials.2011.10.042

Robinson, E. Y., Radziejewski, R. C., Spraggon, C., Greenwald, G., Kostura, J., Burtnick, M. R., ... Jones, S. (1999). The structures of the neurotrophin 4 homodimer and the brain-derived neurotrophic factor/neurotrophin 4 heterodimer reveal a common Trk-binding site. *Protein Science*, 8, 2589–2597. https://doi.org/10.2210/PDB1B8M/PDB

Sakiyama-Elbert, S. E., & Hubbell, J. A. (2000). Controlled release of nerve growth factor from a heparin-containing fibrin-based cell ingrowth matrix. *Journal of Controlled Release*, 69(1), 149–158. https://doi.org/10.1016/S0168-3659(00)00296-0

Santos, D., Gonzalez-Perez, F., Navarro, X., & Del Valle, J. (2016). Dose-dependent differential effect of neurotrophic factors on in vitro and in vivo regeneration of motor and sensory neurons. *Neural Plasticity*, 2016. https://doi.org/10.1155/2016/4969523

Smith, L. E., Bryant, C., Krasowska, M., Cowin, A. J., Whittle, J. D., Macneil, S., & Short, R. D. (2016). Haptotatic plasma polymerized surfaces for rapid tissue regeneration and wound healing. *ACS Applied Materials and Interfaces*, 8, 32675–32687. https://doi.org/10.1021/acsami.6b11320

Stoeckli, E. T., Kuhn, T. B., Duc, C. O., Ruegg, M. A., & Sonderegger, P. (1991). The axonally secreted protein axonin-1 is a potent substratum for neurite growth. *Journal of Cell Biology*, 112(3), 449–455. https://doi.org/10.1083/jcb.112.3.449

Stoeckli, E. T., Lemkin, P. F., Kuhm, T. B., Ruegg, M. A., Heller, M., & Sonderegger, P. (1989). Identification of proteins secreted from axons of embryonic dorsal-root-ganglia neurons. *European Journal of Biochemistry*, 180(2), 249–258. https://doi.org/10.1111/j.1432-1033.1989.tb14640.x

Sumner, A. J. (1990). Aberrant reinnervation. *Muscle & Nerve*, 13, 801–803.

Tang, S., Zhu, J., Xu, Y., Xiang, A. P., Jiang, M. H., & Quan, D. (2013). The effects of gradients of nerve growth factor immobilized PCLA scaffolds on neurite outgrowth invitro and peripheral nerve regeneration in rats. *Biomaterials*, *34*, 7086–7096. https://doi.org/10.1016/j.biomaterials.2013.05.080

Tria, M. A., Fusco, M., Vantini, G., & Mariot, R. (1994). Pharmacokinetics of nerve growth factor (Ngf) following different routes of administration to adult rats. *Experimental Neurology*, *127*, 178–183.

Yan, Q., Yin, Y., & Li, B. (2012). Use new PLGL-RGD-NGF nerve conduits for promoting peripheral nerve regeneration. *Biomedical Engineering Online*, *11*(36), 1–16. https://doi.org/10.1186/1475-925X-11-36

Yang, T., Hussain, A., Bai, S., Khalil, I. A., Harashima, H., & Ahsan, F. (2006). Positively charged polyethylenimines enhance nasal absorption of the negatively charged drug, low molecular weight heparin. *Journal of Controlled Release*, *115*, 289–297. https://doi.org/10.1016/j.jconrel.2006.08.015

Yang, D., Moon, S., & Lee, D. W. (2017). Surface modification of titanium with BMP-2/GDF-5 by a heparin linker and its efficacy as a dental implant. *International Journal of Molecular Sciences*, *18*(229), https://doi.org/10.3390/ijms18010229

Zeng, W., Rong, M., Hu, X., Xiao, W., Qi, F., Huang, J., & Luo, Z. (2014). Incorporation of chitosan microspheres into collagen-chitosan scaffolds for the controlled release of nerve growth factor. *PLoS One*, *9*(7), e101300. https://doi.org/10.1371/journal.pone.0101300

Zhao, Y. Z., Jiang, X., Xiao, J., Lin, Q., Yu, W. Z., Tian, F. R., ... Lu, C. T. (2016). Using NGF heparin-poloxamer thermosensitive hydrogels to enhance the nerve regeneration for spinal cord injury. *Acta Biomaterialia*, *29*, 71–80. https://doi.org/10.1016/j.actbio.2015.10.014

Zhou, Z., & Meyerhoff, M. E. (2005). Preparation and characterization of polymeric coatings with combined nitric oxide release and immobilized active heparin. *Biomaterials*, *26*, 6506–6517. https://doi.org/10.1016/j.biomaterials.2005.04.046

SUPPORTING INFORMATION

Additional supporting information may be found online in the Supporting Information section.

How to cite this article: Sandoval-Castellanos AM, Claeyssens F, Haycock JW. Biomimetic surface delivery of NGF and BDNF to enhance neurite outgrowth. *Biotechnology and Bioengineering*. 2020;1–12. https://doi.org/10.1002/bit.27466